Exploring the half-lives of extremely long-lived α emitters*

Jingya Fan(范敬雅) Chang Xu(许昌)†

School of Physics, Nanjing University, Nanjing 210093, China

Abstract: Naturally occurring α emitters with extremely long half-lives are investigated using the latest experimental data. Within the time-dependent perturbation theory, α decay with a rather narrow width is treated as a quasi-stationary problem by dividing the potential between the α particle and daughter nucleus into a stationary part and a perturbation. The experimental α decay half-lives of seven available long-lived α emitters with $T_{1/2}^{\rm total} > 10^{14}$ y are reproduced with a good accuracy. It is also found that the deformation effect should be treated carefully for long-lived nuclei, especially with low Q_α values. Predictions of the α decay half-lives of twenty naturally occurring nuclei are provided, namely, ^{142}Ce, ^{145,146}Nd, ^{149}Sm, ^{156}Dy, ^{162,164}Er, ^{168}Yb, ^{182,183,184,186}W, ^{187,188,189,190}Os, ^{192,195}Pt, and ^{204,206}Pb. These nuclei are energetically unstable to α decay with low decay energies and extremely long decay half-lives. In particular, the candidates ^{187}Os and ^{149}Sm are strongly recommended for future experiments.

Keywords: alpha decay, half-life, decay mode

DOI: 10.1088/1674-1137/ac500d

I. INTRODUCTION

Alpha radioactivity has been known for a long time as a prevalent decay mode in heavy and superheavy nuclei. Since the pioneering work of Gamow [1], different theoretical methods have been proposed to treat this quasistationary question by solving the time-independent/dependent Schrödinger equation, such as the shell and cluster model [2,3], the S-matrix method [4], the direct method [5], the distorted wave approach [6], and the coupled channel approach [7]. In the quasi-classical limit, the probability of a preformed α particle penetrating through the Coulomb barrier can be approximately calculated by the Wentzel-Kramers-Brillouin (WKB) method [8-23]. Empirical formulas based on the WKB method can also be found in Refs. [24-26]. However, the formation probability of α particles inside the nucleus involves a rather complex many-body (at least five-body) problem [27-32].

Recently, exotic α decay phenomena have attracted much attention owing to the development of experimental facilities and the enhancement of experimental sensitivities. A number of experiments have been devoted to not only the synthesis and identification of new nuclides, such as superheavy nuclei or nuclei far away from the β-stability line [33-35], but also rare α decays with extremely short or long half-lives [36-45]. Experimental data have been accumulated in recent years, which enables us to further improve microscopic decay models and to extend our knowledge of the nuclear force and structure. For instance, a recent experiment on ^{108}Xe→^{104}Te→^{100}Sn [36] by the Argonne National Laboratory (ANL) reported a new record of the fastest α-emitter, ^{104}Te. This extremely short-lived α emitter was investigated in our previous work [14], together with its neighboring nuclei located in the so-called "light island". Several corrections of the α decay data for ^{110}Te, ^{110,112,113}I, ^{113,115}Xe, and ^{112}Cs are recommended [14], and part of these corrections, *i.e.* the α decay branching ratios of ^{110}Te, ^{113}I, and ^{115}Xe, have been adapted in the newest Atomic Mass Evaluation 2020 [46].

Several new experiments have been successfully performed to search for extremely long-lived α emitters during the past decade [37-44]. To date, it is known that the nuclide with the longest α decay half-life is ^{209}Bi with $T_{1/2} = (2.01\pm0.08)\times10^{19}$ y [37,46]. Very recently, the fine structure of ^{209}Bi was measured for the first time and its branching ratio of the ground-state to ground-state α decay is b_α% = (98.8± 0.3)% [37]. Because new experimental data have been accumulated or renewed in recent years, it is interesting to conduct a systematic analysis on the half-lives of available long-lived α emitters. It is also emphasized that there exists a collection of "stable" nuclei with small positive α decay energies [46]. In principle, these nuclei could be succeptible to α particle emission with extremely long half-lives.

Received 29 December 2021; Accepted 29 January 2022; Published online 29 March 2022

* Supported by the National Natural Science Foundation of China (11822503) and the Fundamental Research Funds for the Central Universities (Nanjing University)

† E-mail: cxu@nju.edu.cn, corresponding author

In this work, we firstly explore the possibility of the existence of extremely long-lived α emitters throughout the chart of nuclides. It is found that the nuclei with extremely long half-lives are mainly located in the region between the magic neutron numbers $N = 82$ and $N = 126$ with very low decay energies. Two interesting groups of nuclei are then considered in the present analysis. One group consists of the available long-lived α emitters with $T_{1/2}^{\rm total} > 10^{14}$ y. The other group is made up of nuclei for which α decay is energetically allowed with $Q_\alpha > 1.0$ MeV but has not yet been experimentally observed. Nuclei of both groups are investigated within a time-dependent perturbation theory, namely the two potential approach (TPA). The theoretical α decay half-lives of seven available α emitters with rather long lifetimes are carefully compared with the experimental data. The corresponding wave functions of both favored and unfavored transitions are discussed. Predictions of the α decay half-lives are also given for nuclei for which α decay has not yet been observed. Two possible candidates are recommended for future experiments.

This paper is organized as follows. In Section II, we provide the detailed formulas of the two potential approach for α decay. Section III presents the results on the α decay half-lives and the discussions. A summary is presented in Section IV.

II. FORMULISM OF THE MODIFIED TWO POTENTIAL APPROACH AND NUCLEAR DEFORMATION

Alpha cluster decay, in principle, involves a quasi-stationary problem which is rather difficult to treat in quantum mechanics, especially in the case of deformed nuclei. It is considered that the α cluster decays with an extremely long half-life highly resembles a bound state more than a scattering state. Therefore, a time-dependent perturbation treatment, such as the original or modified two potential approach, can be applied to well define not only the energy shift but also the decay width for α cluster decay. Note that the formation process of the α cluster in nuclei is not touched in the time-dependent perturbation treatment, which is a more complicated quantum few-body problem (at least a five-body problem). Recent microscopic calculation of the α formation problem for ideal Po isotopes with the quartetting wave function provides a solution to the long-standing issue of heavy nuclei [27,29,30]. It is empirically known that the α cluster formation probability P_α, as shown from experimental systematics, differs for even-even, odd-A, and odd-odd nuclei [12,14].

Here we briefly discuss the time-dependent perturbation theory for α cluster decay [8]. The main integrant of TPA is the separation of the α-core potential into two parts at a separation point, $R_{\rm sep}$, where $V(r) = U(r) + W(r)$. The first potential, $U(r)$, and the second potential, $W(r)$, are defined as follows:

$$U(r) = \begin{cases} V(r), & r \le R_{\rm sep} \\ V(R_{\rm sep}) = V_0, & r > R_{\rm sep} \end{cases},$$
$$W(r) = \begin{cases} 0, & r \le R_{\rm sep} \\ V(r) - V_0, & r > R_{\rm sep} \end{cases}. \quad (1)$$

The α cluster is first considered to stay in the bound state, $\Phi_0(r)$, of the Hamiltonian $\widehat{H}_0 = -\hbar^2\nabla^2/2\mu + U(r)$ with eigenvalue, E_0. Here, μ is the reduced mass of the α particle and daughter nucleus. This bound state transforms to a quasi-stationary state by switching on the second potential, $W(r)$, at $t = 0$ [8]. The eigenvalue, E, of the quasi-stationary state can be obtained from the complex-energy pole of the total Green's function, $G(E) = \left[E - \widehat{H}\right]^{-1}$, with $\widehat{H} = -\hbar^2\nabla^2/2\mu + V(r)$. The energy shift $\Delta = {\rm Re}(\varepsilon_0)$ and width $\Gamma = -2{\rm Im}(\varepsilon_0)$ of the quasi-stationary state can be given by

$$\varepsilon_0 = E - E_0 = \langle\Phi_0|W|\Phi_0\rangle + \langle\Phi_0|W\widetilde{G}(E)W|\Phi_0\rangle. \quad (2)$$

Here an iterative form is presented for $\widetilde{G}(E)$ that $\widetilde{G}(E) = G_0(E)[1 + \widetilde{W}(r)\widetilde{G}(E)]$ with $\widetilde{W}(r) = W(r) + V_0$ and $G_0(E) = \dfrac{1-\Lambda}{E + V_0 - \widehat{H}_0}$, where $\Lambda = |\Phi_0\rangle\langle\Phi_0|$ [8]. Note that all the above derivations are general, but the numerical solution of $\widetilde{G}(E)$is quite difficult. To make it feasible within the current capacity of computer calculation, $\widetilde{G}(E)$is replaced approximately with $G_{\widetilde{W}}(E_0)$ [8]. Thus, the decay width, Γ, is given as

$$\Gamma = \frac{4\hbar^2\alpha^2}{\mu k}\left|\Phi_0(r)\chi_k(r)\right|^2_{r=R_{\rm sep}}, \quad (3)$$

where $k = \sqrt{2\mu E_0}/\hbar$ and $\alpha = \sqrt{2\mu[V_0 - E_0]}/\hbar$. $\chi_k(r)$ is the eigenfunction of the Schrödinger equation for $\widetilde{W}(r)$. For detailed discussions and evaluations on the correction terms from the above approximation, please see Ref. [8]. It is concluded in Ref. [47] that, to minimize the correction terms, the separation radius, $R_{\rm sep}$, should be taken far away from the inner turning point, r_2, but not too close to the outer turning point, r_3. Once this condition is satisfied, the result of Γ could be weakly dependent on $R_{\rm sep}$. Thus, to obtain the α decay width, Γ, the wave functions $\Phi_0(r)$ and $\chi_k(r)$ at $R_{\rm sep}$, well inside the barrier, should be evaluated. When the WKB wave functions are applied for $\Phi_0(r)$ and $\chi_k(r)$, a quasi-classical decay width can be further deduced: $\Gamma = \dfrac{\hbar^2 N}{4\mu}\exp\left[-2\int_{r_2}^{r_3}\sqrt{2\mu|E_0 - V(r)|}/\hbar{\rm d}r\right]$. Here, N is a normalization factor. This formula re-

sembles the formula of the Gamow model [1],$\Gamma = A\exp[-S/\hbar]$, but with a well-defined preexponential factor, A. This is the merit of the perturbation treatment that one can now define the classic concept "frequency of collision" or the so-called preexponential factor with the corresponding wave functions [8].

It has been previously found that the deformation of nuclei could result in a significant influence on the α decay width. A simplified approach is to assume an α particle interacting with the axially deformed daughter nucleus, and an averaging procedure is applied to obtain the α decay width along different orientation angles [12]. In principle, the α decaying state should be described by a three-dimensional quasi-stationary state wave function. However, the three-dimensional TPA is rather complex to handle, as the accurate information of the wave function at a large distance is required. In this work, we follow the averaging procedure to obtain the α decay width by using the deformed Woods-Saxon (WS) potential and Coulomb potential. The depth of the WS potential is adjusted to reproduce the experimental decay energy, Q_α , and nodes of the wave function, n, determined by the Wildermuth condition, $G = 2n + l$ [48]. Other potential parameters are the same as those in the previous study [49]. Once the total α-core potential has been determined, the bound state wave function, $\Phi_0(r)$ for $U(r,\theta)$, is obtained by numerically solving the radial Schrödinger equation at each θ. Furthermore, the scattering wave function, $\chi_k(r)$, is the linear combination of the regular and irregular Coulomb functions. The angle-dependent decay width, $\Gamma(\theta)$, is then calculated by using Eq. (3). The total α decay width is obtained by averaging $\Gamma(\theta)$ in all directions as $\Gamma_{\rm total} = \frac{1}{2}\int_0^\pi \Gamma(\theta)\sin\theta {\rm d}\theta$. The half-life can be calculated using the following relation:

$$T_{1/2} = \frac{\hbar \ln 2}{P_\alpha \Gamma_{\rm total}}. \tag{4}$$

Systematic analyses of α transitions show that the variation of the α-cluster preformation probability, P_α , is small for open-shell nuclei, where a set of constant values, namely $P_\alpha = 0.38$ for even-even nuclei, $P_\alpha = 0.24$ for odd-A nuclei, and $P_\alpha = 0.13$ for odd-odd nuclei [12], can be applied in the calculations on the α decay half-lives. However, for nuclei in closed-shell regions, the clustering of the nucleons is strongly hindered. For example, P_α of ^{209}Bi is reduced to a much smaller value as $P_\alpha = 0.03$ [50] considering the strong shell effect ($N = 126$) and Pauli blocking effect.

III. RESULTS AND DISCUSSION

Before giving the detailed results of our calculation with TPA, we first discuss the criteria for selecting the nuclei. In Fig. 1, we plot all the experimental α decay energies of nuclei throughout the mass region, $80 \le A \le 260$ [51]. The stable nuclides are marked by black circles. The gray curve represents the nuclei on the β-stability line, empirically formulated by $Z = \frac{A}{1.98+0.0155A^{2/3}}$ as given in textbooks [52]:

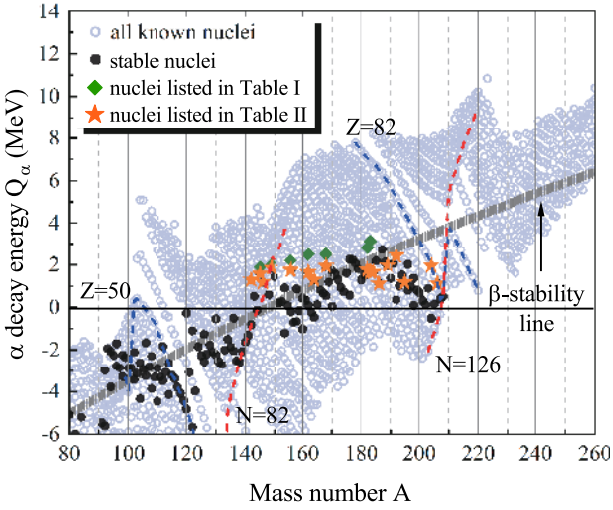

Fig. 1. (color online) α decay energy Q_α of nuclei in the mass region, $80 \le A \le 260$. Green diamonds and orange stars denote the two groups of nuclei investigated in this work. The proton magic numbers $Z = 50, 82$ and the neutron magic numbers $N = 82, 126$ are indicated by blue dash lines and red dash lines, respectively.

$$Q_\alpha = \frac{48.88}{A^{1/3}} - 92.80\left(1 - \frac{2Z}{A}\right)^2 + 2.856\frac{Z}{A^{1/3}}\left(1 - \frac{Z}{3A}\right) - 35.04\ {\rm MeV}. \tag{5}$$

Then, all the α emitters with experimental total half-lives longer than 10^{14} y are selected, *i.e.,* ^{144}Nd, ^{148}Sm, ^{152}Gd, ^{174}Hf, ^{180}W, ^{186}Os, and ^{209}Bi (see green diamonds in Fig. 1). Naturally occurring isotopes of Ce, Nd, Sm, Dy, Er, Yb, W, Os, Pt, and Pb, which are marked as "stable" in AME2020 [46], are also presented in Fig. 1 as orange stars. An important feature of these long-lived nuclei is that their α decay energies are quite low ($1.0{\rm MeV} < Q_\alpha < 3.2{\rm MeV}$). It is also noticed that these nuclei are mainly located in the region between the magic neutron numbers $N = 82$ and $N = 126$. The theoretical α decay half-lives of the two groups of nuclei are listed in Table 1 and Table 2, respectively.

In Table 1, we present a comparison between the experimental and theoretical α decay half-lives for seven extremely long-lived α emitters. For these nuclei with rather low decay energies ranging from 1.9 MeV to 3.2 MeV, the theoretical half-lives, T_α , agree reasonably with the experimental data. The largest deviation between data and theory is reported for ^{174}Hf, whose daughter

Table 1. Experimental and theoretical α decay half-lives for extremely long-lived α emitters. The isotopic abundance, IS; the α decay branching ratio, b_α%, from ground state to ground state ($g.s. \to g.s.$); the α decay energy, Q_α; and the experimental α decay half-life, $T_\alpha^{\rm Exp}$, are taken from AME2020 [46]. β_2 and β_4 denote the quadrupole and hexadecapole deformation parameters corresponding to the daughter nucleus [53]. l is the minimum orbital angular momentum carried by the α particle, and G is the global number.

Nuclide	IS(%)	b_α %	Q_α/MeV	β_2	β_4	l	G	$T_\alpha^{\rm Exp}$/y	$T_\alpha^{\rm Cal}$/y
^{144}Nd	23.789(19)	100	1.901	0.000	0.000	0	18	$(2.29\pm0.16)\times10^{15}$	1.13×10^{16}
^{148}Sm	11.25(9)	100	1.987	0.000	0.000	0	18	$(6.3\pm1.3)\times10^{15}$	2.56×10^{16}
^{152}Gd	0.20(3)	100	2.204	0.172	0.060	0	18	$(1.08\pm0.08)\times10^{14}$	2.07×10^{14}
^{174}Hf	0.16(12)	100	2.494	0.287	−0.018	0	18	$(2.0\pm0.4)\times10^{15}$	2.59×10^{16}
^{180}W	0.12(1)	100	2.515	0.278	−0.057	0	18	$(1.59\pm0.05)\times10^{18}$	6.24×10^{17}
^{186}Os	1.59(64)	100	2.821	0.232	−0.066	0	18	$(2.0\pm1.1)\times10^{15}$	1.49×10^{15}
^{209}Bi	100	98.8	3.137	0.000	0.000	5	21	$(2.03\pm0.08)\times10^{19}$	6.89×10^{18}

Table 2. Predicted α decay half-lives for twenty possible α emitters with rather low decay energies. The current half-life limit, isotopic abundance (IS), decay modes, and α decay energies, Q_α , are taken from AME2020 [46]. The deformation parameters β_2 and β_4 of the daughter nuclei are taken from Ref. [53]. l is the minimum orbital angular momentum carried by the α particle, and G is the global number.

Nuclide	Half-life	IS(%)	Decay modes	Q_α/MeV	β_2	β_4	l	G	$T_\alpha^{\rm Cal}$/y
^{142}Ce	>2.9 Ey	11.114(51)	$\alpha?;2\beta^-?$	1.304	0.000	0.000	0	18	1.76×10^{28}
^{145}Nd	>60 Py	8.293(12)	$\alpha?$	1.574	−0.032	0.000	0	18	1.73×10^{23}
^{146}Nd	>1.6 Ey	17.189(32)	$2\beta^-?;\alpha?$	1.182	0.011	0.000	0	18	1.06×10^{35}
^{149}Sm	>2 Py	13.82(10)	$\alpha?$	1.871	0.109	0.030	0	18	4.80×10^{18}
^{156}Dy	>1 Ey	0.056(3)	$\alpha?;2\beta^+?$	1.753	0.205	0.053	0	18	6.35×10^{24}
^{162}Er	>140 Ty	0.139(5)	$\alpha?;2\beta^+?$	1.648	0.260	0.063	0	18	1.70×10^{29}
^{164}Er		1.601(3)	$\alpha?;2\beta^+?$	1.305	0.272	0.053	0	18	8.29×10^{39}
^{168}Yb	>130 Ty	0.123(3)	$\alpha?;2\beta^+?$	1.938	0.284	0.018	0	18	2.80×10^{24}
^{182}W	>7.7 Zy	26.50(16)	$\alpha?$	1.764	0.278	−0.071	0	18	4.01×10^{32}
^{183}W	>670 Ey	14.31(4)	$\alpha?$	1.673	0.267	−0.073	5	19	4.69×10^{36}
^{184}W	>8.9 Zy	30.64(2)	$\alpha?$	1.649	0.267	−0.086	0	18	5.49×10^{35}
^{186}W	>4.1 Ey	28.43(19)	$2\beta^-?\alpha?$	1.116	0.268	−0.099	0	18	1.42×10^{56}
^{187}Os	>3.2 Py	1.96(17)	$\alpha?$	2.722	0.243	−0.078	0	18	4.57×10^{16}
^{188}Os	>3.3 Ey	13.24(27)	$\alpha?$	2.143	0.232	−0.093	0	18	1.11×10^{26}
^{189}Os	>3.3 Py	16.15(23)	$\alpha?$	1.976	0.221	−0.094	0	18	6.04×10^{29}
^{190}Os	>12 Ey	26.26(20)	$\alpha?$	1.376	0.221	−0.095	0	18	1.64×10^{47}
^{192}Pt	>60 Py	0.782(24)	$\alpha?$	2.424	0.198	−0.085	0	18	5.57×10^{22}
^{195}Pt	>6.3 Ey	33.775(240)	$\alpha?$	1.176	0.164	−0.077	4	18	8.66×10^{59}
^{204}Pb	>140 Py	1.4(6)	$\alpha?$	1.969	−0.094	−0.020	0	18	8.42×10^{35}
^{206}Pb	>2.5 Zy	24.1(30)	$\alpha?$	1.135	−0.073	−0.007	0	18	3.42×10^{66}

The units of half-life are Ty: 10^{12} y, Py: 10^{15} y, Ey: 10^{18} y, and Zy: 10^{21} y, respectively [46].

nucleus is a largely deformed one with $\beta_2 = 0.287$ and $\beta_4 = -0.018$. This deformation results in a reduction of approximately 70% in the half-life of ^{174}Hf as compared with the spherical assumption ($\beta_2 = 0$ and $\beta_4 = 0$). In Fig. 2, we illustrate the ratios of α decay half-lives in the deformed and spherical cases as a function of α decay energy. For comparison, the ^{152}Gd is also selected, whose daughter nucleus is moderately deformed with $\beta_2 = 0.172$ and $\beta_4 = 0.060$. It can be clearly seen that the ratios for ^{152}Gd and ^{174}Hf are all smaller than 1, indicating that the half-lives of these two α emitters are decreased by the deformation; the larger the deformation, the stronger the ef-

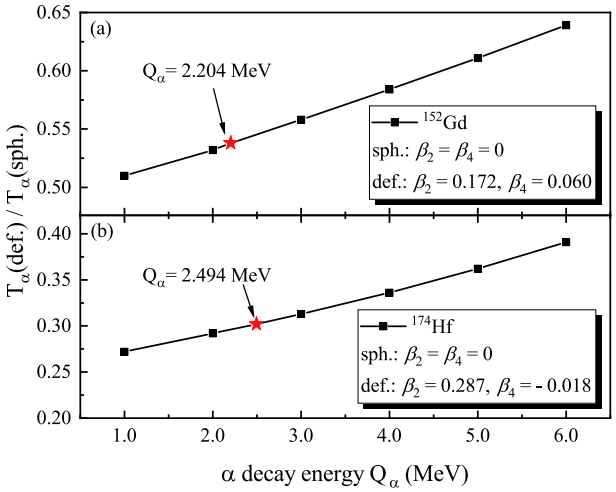

Fig. 2. (color online) Ratios of the α decay half-lives in the deformed case, T_α(def.), to those in the spherical case, T_α(cal.), as a function of the α decay energy Q_α for ^{152}Gd and ^{174}Hf. Experimental values are indicated by red stars.

fect. It is also found that the ratios T_α(def.)/T_α(sph.) decrease with decreasing Q_α. Thus, for long-lived nuclei with low α decay energies, one should be careful to describe the deformation effect. By better treating the averaging procedure along different angles, it is expected that the agreement for largely deformed nuclei can be further improved. In addition, the α cluster formation factor, P_α, could also vary with the deformation degree of freedom. Here, the P_α values are assumed to be the same for both spherical and deformed nuclei.

Another factor that should be taken into account is the angular momentum carried by the α particle. As shown in Table 1, six favored α transitions with $l = 0$ are involved. The only exception is ^{209}Bi with a large angular momentum, $l = 5$. For this unfavored α decay, both the height and width of the Coulomb barrier are significantly increased by its centrifugal potential. The ratio of the corresponding decay width, Γ, with $l = 5$ to $l = 0$ for ^{209}Bi is $\frac{\Gamma_{l=5}}{\Gamma_{l=0}} \approx 0.05$. It should be interesting to discuss the correlation between the α-core potential and the corresponding bound state wave function of the α particle for both favored and unfavored cases. The potentials and wave functions of ^{209}Bi$\rightarrow^{205}$Tl+α and ^{148}Sm$\rightarrow^{144}$Nd+α are plotted for better illustration. As shown in Fig. 3(a), there exists a strong repulsive behavior of the potential, $U(r)$, for ^{209}Bi in the inner part due to the angular momentum $l = 5$. Consequently, the corresponding bound state wave function, $\Phi_0(r)$, of ^{209}Bi is pushed outwards compared with that of ^{148}Sm, as presented in Fig. 3(b). Oscillations of the two wave functions are quite similar when $r < R_{\rm sep}$, but the node numbers of $\Phi_0(r)$ for ^{209}Bi (blue line) and ^{148}Sm (red chain-dotted line) are $n = 8$ and $n = 9$, respectively. The decay of ^{209}Bi involves a higher Coulomb barrier in the classically forbidden region. To be more specific, there is a difference of 3–4 MeV of $U(r)$ for ^{209}Bi and ^{148}Sm at $r = R_{\rm sep}$. As a result, one can see from the right panel of Fig. 3(b) that the bound state wave functions for these two nuclei decrease exponentially in the outer region ($r \geq R_{\rm sep}$), and $\Phi_0(r)$ for ^{209}Bi decreases more quickly due to the differences between the Coulomb barriers of the two nuclei.

For the twenty selected long-lived nuclei, the predicted α decay half-lives, T_α , calculated using the latest nuclear mass data [46] are listed in Table 2. The second, third, and fourth columns in Table 2 present the current half-life limit, isotopic abundance (IS), and possible decay modes for each nucleus [46]. Listed in the fifth column are the α decay energies taken from Ref. [46].

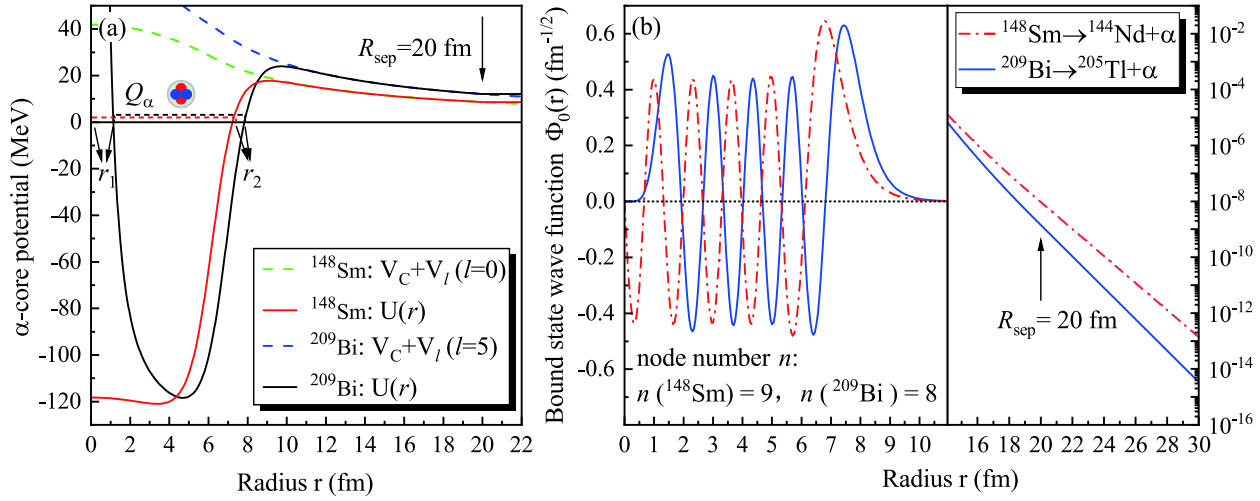

Fig. 3. (color online) α-core potentials (a) and corresponding bound state wave functions (b) for ^{148}Sm$\rightarrow^{144}$Nd+α and ^{209}Bi$\rightarrow^{205}$Tl+α, respectively. The separation point, $r = R_{\rm sep}$, is indicated both in (a) and (b). r_1 and r_2 in (a) are the first and second classical turning points, respectively.

One can find that the α decay energies of the nuclei are in the range of 1.0 MeV$< Q_\alpha <$ 2.8 MeV. Among them, ^{187}Os is found to have the largest α decay energy with Q_α = 2.722 MeV. It is well-known that the decay width is closely dependent on the decay energy, and the larger the decay energy, the easier the penetration of the preformed α cluster through the Coulomb barrier. The sixth and seventh columns present the deformation parameters of the daughter nuclei. As shown in Table 2, all nuclides except ^{142}Ce investigated here decay to a deformed nucleus since they are located in the open-shell region between the magic neutron numbers N = 82 and N = 126. In particular, the nuclei with mass numbers ranging from A = 160 to A = 190 are largely deformed (^{162}Er–^{190}Os). Similarly, the deformation effects are taken into account in the calculation through the averaging procedure. A 100% *g.s.* to *g.s.* transition is assumed since the values of branching ratio, b_α%, are unknown. The predicted α decay half-lives are then given, which vary by several orders of magnitude from 10^{16} y to 10^{66} y. The fastest one among these possible α emitters is ^{187}Os, for which the predicted α decay half-life is $T_\alpha = 4.57\times10^{16}$ y. However, the isotopic abundance of ^{187}Os is rather low (IS = 1.96%), which adds another layer of difficulty in observing the α decay events. As compared with ^{187}Os, ^{149}Sm is more abundant with IS = 13.82%, for which the predicted α decay half-live is $T_\alpha = 4.80\times10^{18}$ y. For other nuclides, the predicted α decay half-lives are many orders of magnitude longer than the theoretical T_α of ^{187}Os and ^{149}Sm. It can be quite difficult to observe their α decays with the present experimental sensitivities. Thus, ^{187}Os and ^{149}Sm are recommended for future experiments searching for new long-lived α emitters.

Finally, it is worth noting that the calculation of the α decay width for deformed nuclei within the averaging procedure is an approximate treatment. Several other approaches for α decay of deformed nuclei can be applied, such as the coupled channel approach or the α-plus-rotor model. In general, the α decaying state of deformed nuclei should be described by a three-dimensional quasi-stationary state wave function. A multidimensional approach should be developed for the tunneling of the α particle through a deformed Coulomb barrier. For instance, one can solve a three-dimensional Schrödinger equation to obtain the decay width, Γ, by a number of methods: (i) grid-based approach [54], (ii) imaginary time propagation method [55] (iii), basis expansion method [56], *etc*. However, the solution of the three-dimensional Schrödinger equation is quite complex and limited by the matrix size or the number of bases. For wave functions at large separation, $r = R_{\rm sep}$, the computation procedure could be rather time-consuming. The calculation providing a solution to the three dimensional α decay is undergoing.

IV. SUMMARY

The α decay half-lives of naturally occurring nuclei with extremely long half-lives are investigated with the latest experimental data. By using the two potential approach, the narrow α decay width is expressed as a product of the bound state and scattering state wave functions of the α particle. The half-lives of α emitters are significantly decreased due to the deformations of the daughter nuclei, especially for low decay energy, Q_α. For available long-lived α emitters with rather low decay energies, the agreement between the theoretical α decay half-lives and the experimental data is reasonable. Moreover, the α decay half-lives of twenty candidates with low decay energies are predicted, for which α decays are energetically allowed but have not yet been observed. In particular, ^{187}Os is found to have the shortest α decay half-life with $T_\alpha = 4.57\times10^{16}$ y, followed by ^{149}Sm with $T_\alpha = 4.80\times10^{18}$ y. It is considered that the observations of α decays for both ^{187}Os and ^{149}Sm are within the current experimental possibilities, which are strongly recommended for future experiments.

References

[1] G. Gamow, Z. Phys. **51**, 204 (1928)
[2] K. Varga, R. G. Lovas, and R. J. Liotta, Phys. Rev. Lett. **69**, 37 (1992)
[3] D. S. Delion, *Theory of particle and cluster emission* (Springer-Verlag, Berlin, 2010)
[4] M. L. Goldberger and K. M. Watson, Phys. Rev. **136**, B1472 (1964)
[5] E. Maglione, L. S. Ferreira, and R. J. Liotta, Phys. Rev. Lett. **81**, 538 (1998)
[6] S. Åberg, P. B. Semmes, and W. Nazarewicz, Phys. Rev. C **56**, 1762 (1997)
[7] D. S. Delion, S. Peltonen, and J. Suhonen, Phys. Rev. C **73**, 014315 (2006)
[8] S. A. Gurvitz, Phys. Rev. A **38**, 1747 (1988); S. A. Gurvitz and G. Kalbermann, Phys. Rev. Lett. **59**, 262 (1987).
[9] B. Buck, A. C. Merchant, and S. M. Perez, Phys. Rev. Lett. **65**, 2975 (1990)
[10] G. Royer, J. Phys. G: Nucl. Part. Phys. **26**, 1149 (2000)
[11] Chang Xu and Zhongzhou Ren, Phys. Rev. C **69**, 024614 (2004)
[12] Chang Xu and Zhongzhou Ren, Phys. Rev. C **74**, 014304 (2006)
[13] Dongdong Ni and Zhongzhou Ren, Phys. Rev. C **80**, 051303 (2009)
[14] Jingya Fan and Chang Xu, Nucl. Phys. A **989**, 1-12 (2019)
[15] W. M. Seif and A. Abdurrahman, Chin. Phys. C **42**, 014106 (2018)
[16] Dong Bai and Zhongzhou Ren, Chin. Phys. C **42**, 124102 (2018)

[17] Hong-Ming Liu, You-Tian Zou, Xiao Pan *et al*., Chin. Phys. C **44**, 094106 (2020)
[18] Yan He, Xuan Yu, and Hongfei Zhang, Chinese Phys. C **45**, 014110 (2021)
[19] Na-Na Ma *et al*., Chin. Phys. C **45**, 024105 (2021)
[20] Zhishuai Ge *et al*., Chin. Phys. C **44**, 104102 (2020)
[21] Jun-Gang Deng *et al*., Chin. Phys. C **41**, 124109 (2017)
[22] Gao-Long Zhang and Xiao-Yun Le, Chin. Phys. C **33**, 354-358 (2009)
[23] Yibin Qian and Zhongzhou Ren, Chin. Phys. C **45**, 021002 (2021)
[24] Lu-Lu Li, Shan-Gui Zhou, En-Guang Zhao *et al*., Int. J. Mod. Phys. E **19**, 359 (2010)
[25] S. S. Hosseini and H. Hassanabadi, Chin. Phys. C **41**, 064101 (2017)
[26] Jin-Song Peng *et al*., Chin. Phys. C **32**, 634-638 (2008)
[27] G. Röpke, P. Schuck, Y. Funaki *et al*., Phys. Rev. C **90**, 034304 (2014)
[28] Chang Xu, G. Röpke, P. Schuck *et al*., Phys. Rev. C **93**, 011306(R) (2016)
[29] Chang Xu, G. Röpke, P. Schuck *et al*., Phys. Rev. C **95**, 061306 (2017)
[30] Shuo Yang, Chang Xu, G. Röpke *et al*., Phys. Rev. C **101**, 024316 (2020)
[31] Shuo Yang, Chang Xu, and G. Röpke, Phys. Rev. C **104**, 034302 (2021)
[32] C. Qi, R. Liotta, and R. Wyss, Prog. Part. Nucl. Phys. **105**, 214-251 (2019)
[33] Z. Y. Zhang, Z. G. Gan, H. B. Yang *et al*., Phys. Rev. Lett. **122**, 192503 (2019)
[34] Z. Y. Zhang, H. B. Yang, M. H. Huang *et al*., Phys. Rev. Lett. **126**, 152502 (2021)
[35] Wei Hua *et al*., Chin. Phys. C **45**, 044001 (2021)
[36] K. Auranen *et al*., Phys. Rev. Lett. **121**, 182501 (2018)
[37] J. W. Beeman *et al*., Phys. Rev. Lett. **108**, 062501 (2012)
[38] P. Belli *et al*., Nucl. Instrum. Methods A **626-627**, 31-38 (2011)
[39] J. W. Beeman *et al*., Eur. Phys. J. A **49**, 50 (2013)
[40] H. Wilsenach *et al*., Phys. Rev. C **95**, 034618 (2017)
[41] M. Braun *et al*., Phys. Lett. B **768**, 317 (2017)
[42] P. Belli *et al*., Phys. Rev. C **83**, 034603 (2011)
[43] F. A. Danevich *et al*., Eur. Phys. J. A **56**, 5 (2020)
[44] P. Belli *et al*., Phys. Rev. C **102**, 024605 (2020)
[45] P. Belli, R. Bernabei, F. A. Danevich *et al*., Eur. Phys. J. A **55**, 140 (2019)
[46] F. G. Kondev, M. Wang, W. J. Huang *et al*., Chin. Phys. C **45**, 030001 (2021)
[47] S. A. Gurvitz, P. B. Semmes, W. Nazarewicz *et al*., Phys. Rev. A **69**, 042705 (2004)
[48] K. Wildermuth and Y. C. Tang, *A Unified Throey of the Nucleus* (Academic Press, New York, 1977)
[49] Yibin Qian, Zhongzhou Ren, and Dongdong Ni, Phys. Rev. C **83**, 044317 (2011)
[50] Chang Xu and Zhongzhou Ren, Phys. Rev. C **68**, 034319 (2003)
[51] *https://nds.iaea.org*
[52] Xi-Ting Lu *et al*., Nuclear Physics (*in Chinese*), (Atomic Energy Press, 2000), p. 119
[53] P. Möller, A. J. Sierk, T. Ichikawa *et al*., At. Data Nucl. Data Tables **1**, 109-110 (2016)
[54] T. Graen, H. Grubmüller, Comput. Phys. Commun. **198**, 169-178 (2016)
[55] S. A. Chin, S. Janecek, and E. Krotscheck, Comput. Phys. Commun. **180**, 1700-1708 (2009)
[56] A. T. Kruppa and Z. Papp, Comput. Phys. Commun. **36**, 59-78 (1985)